

HIGH LINEARITY CMOS VARIABLE GAIN AMPLIFIER FOR UWB APPLICATIONS

I. L. Abdel-Hafez¹, Y. A. Khalaf², and F. A. Farag^{3,*}

*Electronics and Communications Dept., Faculty of Engineering,
Zagazig University, Zagazig, Egypt*

Received 11 November 2012; accepted 11 December 2012

ABSTRACT

A large dynamic-range Variable Gain Amplifier (VGA) suitable for Ultra Wide Band (UWB) applications is presented. The VGA is composed of three programmable variable gain amplifier stages followed by an output buffer. Such wide bandwidth allows our proposed VGA to be used in multi-standard protocols. Power reduction is developed for the variable gain amplifier stages. Thorough analyses of the mid-band gain and noise are presented; and design tradeoffs are carefully handled. The VGA circuit is designed and simulated in 0.13 μm IBM-CMOS process; the overall VGA with buffer consumes 25 mA from a 1.5 V supply. The VGA achieves 54.5 dB dynamic-range (DR), 17.6 dBm IIP3, -42.31 dB THD at peak-to-peak differential output voltage of 1 V, and frequency 400 MHz. Moreover; the proposed circuit reports a good noise performance; the average integrated noise is 121.6 nV/ $\sqrt{\text{Hz}}$ at minimum gain of -0.5 dB.

Keywords: Automatic Gain Control (AGC), Variable Gain Amplifier (VGA), Digitally-controlled Variable Gain Amplifier (DVGA), Buffer, CMOS Analog Integrated Circuits, Low Voltage, Wide Bandwidth.

1. Introduction

The variable gain amplifier (VGA) is an indispensable building block to maximize the dynamic range of modern wireless communication systems [1], [2]. It is also widely used in medical equipment, hearing aids, disk drives, and so on [3]–[5]. A VGA is typically employed in a feedback loop to realize automatic gain control (AGC). The VGA of an AGC loop is used to control the transmission signal power or to adjust the received signal amplitude. There are two possible approaches to control the gain of the VGA. One is to build a discrete gain step VGA with a digital control signal [6], [7]; and the other is to design a VGA controlled by an analog gain- control signal [1]–[5]. Basically, digitally-controlled VGAs use binary weighted arrays of resistors or capacitors for gain variations whereas analog-controlled VGAs adopt a variable transconductance or a variable resistance to control the gain. VGA circuits based on various technologies such as bipolar, BiCMOS, and CMOS have been introduced in the literature (e.g. [1]–[4]).

An important VGA requirement is to have a linear-in-decibel gain control characteristic, where the gain of the VGA changes exponentially with the control signal. The exponential gain control is required to achieve a wide dynamic-range and to maintain the AGC loop settling-time independent of the input signal level [8].

* Corresponding author.

E-mail: FFARAG@ZU.EDU.EG

Another important aspect of a wideband VGA is to attain a large bandwidth. There are many systems for high-speed data communications such as ultra-wideband (UWB) systems, wireless local area networks (LANs), and Bluetooth. These systems provide a high data rate with relatively low power consumption in short-range wireless communications. For high-speed data communication, the bandwidth of a VGA must be very wide. Therefore, a wideband VGA is a key component.

While the density of the devices in Nanoscale technology is continually increasing, the interconnect lines across a chip increase significantly. Such long interconnects mandate the requirement of driving large capacitances [12]-[15]. Moreover, in some situations, circuits should have large fan-out. For these reasons, buffers are frequently used in analog and mixed signal circuits. Well-designed buffers should drive large capacitive load with wide bandwidth, minimum power consumption, low distortion, and low loading effect.

In this paper, we propose a new highly-linear wideband variable gain amplifier VGA. Our VGA parameters are compared to [17] – [20] to clarify the merits of the proposed circuit. It could obtain a high linearity, wide bandwidth, and large dynamic-range with large capacitive load and high swing.

Section II describes the architecture of the proposed wideband VGA supported by VGA-cell analysis. The design of the main blocks in the VGA is also explained. Noise and linearity performance of the VGA are analyzed. The implementation and simulation results are presented in Section III. The results are also analyzed and discussed. Conclusions are given in section IV.

2. Wideband CMOS variable gain amplifier

The proposed variable gain amplifier VGA, as shown in **Fig. 1**, consists of a number of variable gain amplifier stages (cells) followed by a buffer to drive the load. A binary control-word is used to control the gain of the variable gain amplifiers. The bandwidth of such variable gain amplifier cell should be so wide that the overall bandwidth of the whole VGA design is achieved. In this section, we introduce a three-stage configuration to implement the VGA with wide bandwidth, in which all VGA-cells are identical. The Variable Gain Amplifier (VGA)-cells implementation is considered and analyzed here. A novel VGA-cell, based on the Flipped Voltage Follower (FVF) [11] technique, is proposed with modifications to increase the headroom for the output swing and to enhance the transconductance of the VGA-cell. A new topology for the output buffer is also described and analyzed.

2.1. Variable gain amplifier cell

The complete circuit of the proposed VGA-cell is shown in **Fig. 2**. It demonstrates the signal-processing circuit, the common-mode-feedback circuit, and the bias circuit.

The VGA-cell consists of a CMOS differential amplifier, in which the R_f and R_s are used to vary the gain. C_s is inserted to widen out the bandwidth. M_1 and M_2 are used to transfer the differential-voltage signal across R_s , which in turn is converted into differential-current flowing through M_3 and M_4 . The differential signal current is mirrored to the output branches through M_5 and M_6 . M_7 and M_8 are connected in Wilson current-mirror like-connectivity to define drain voltage of M_1 and M_2 ; and to provide larger headroom for the swing at these points in contrast to [11]. It also provides large output resistance at the output nodes V_{OP} and V_{OM} . This VGA-cell is typically used to get the coarse and fine steps by controlling R_s and R_f , respectively.

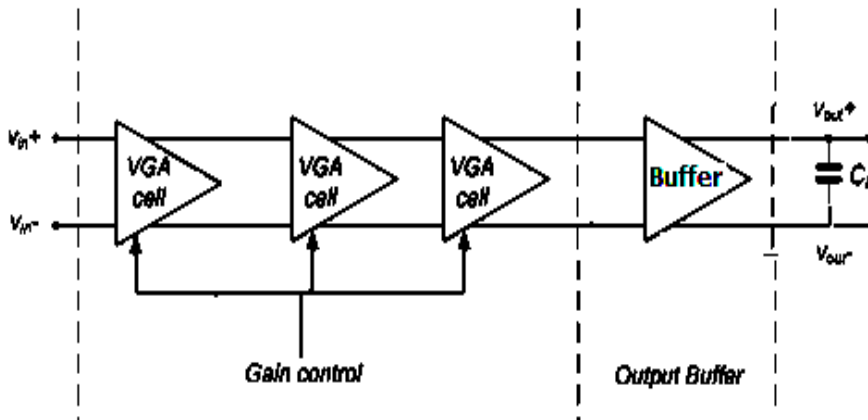


Fig. 1. Architecture of the overall VGA.

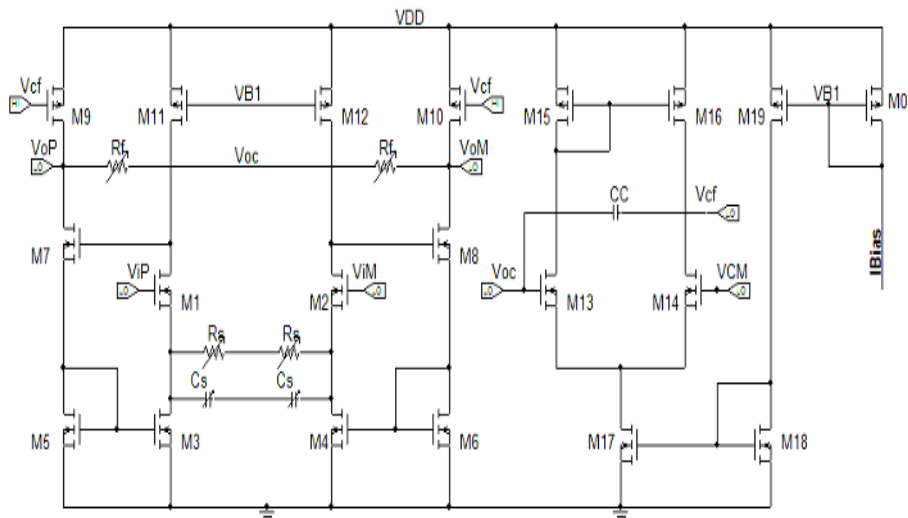


Fig. 2. Schematic diagram of the proposed VGA-cell.

The output voltage (V_{OP}) half-circuit of the low-frequency small-signal model for the differential amplifier is shown in **Fig. 3**. The output voltage can be written as,

$$V_{oP} = -g_{m5}V_{gs3}(R_f // r_{o9}) \quad (1)$$

where g_{m5} is the transconductance of M_{5-6} , V_{gs3} is the voltage between gate and source of $M_{3,4}$, and r_{o9} is the output resistance of the transistor M_{9-10} . r_{o5} is ignored, compared to $1/g_{m5}$. The input voltage V_{iP} of the differential amplifier is then,

$$V_{iP} = V_{gs1} + (I - g_{m3}V_{gs3})(R_s // r_{o3}) \quad (2)$$

where I is the current flowing into r_{o11} .

$$I = \frac{g_{m1}r_{o1}V_{gs1} + g_{m3}(R_s // r_{o3})V_{gs3}}{[(R_s // r_{o3}) + r_{o1} + r_{o11}]} \quad (3)$$

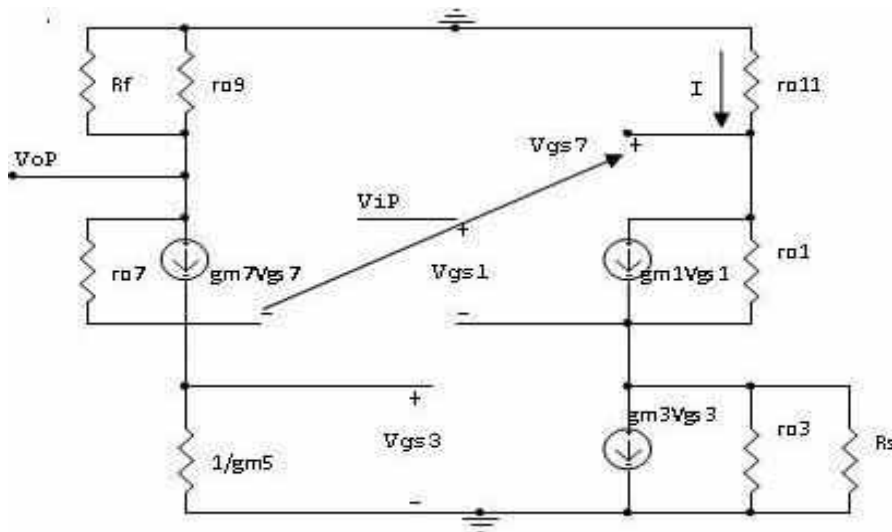


Fig. 3. Small-signal model of VGA circuit.

Applying KVL on the output branch, V_{gs7} can be calculated as,

$$V_{gs7} = \frac{[1 + g_{m5}(r_{o7} + (R_f // r_{o9})]V_{gs3}}{g_{m7}r_{o7}} \quad (4)$$

On the other hand, V_{gs3} can be related to V_{gs7} as,

$$V_{gs3} + V_{gs7} = -I r_{o11} \quad (5)$$

Using equations (1) through (5) and doing some mathematical manipulation, we can calculate the output voltage gain A_V :

$$A_V \equiv \frac{V_{oP}}{V_{iP}} = \frac{(R_f // r_{o9})}{(R_s // r_{o3})} \left[\frac{1}{\left(\frac{g_{m3}}{1 + \frac{g_{m5}}{r_{o1} + r_{o11}}} \right) + \left[\frac{X}{A} \right] \left(1 + \frac{g_{m1} r_{o1} (R_s // r_{o3})}{g_{m5} (R_s // r_{o3})} \right)} \right] \quad (6)$$

r_{o11} represents the resistance of the current source. If r_{o11} is relatively large, the output voltage gain A_V can be approximated as,

$$A_V \equiv \frac{V_{oP}}{V_{iP}} = \frac{(R_f // r_{o9})}{(R_s // r_{o3})} \frac{g_{m5}}{g_{m3}} \quad (7)$$

It is worthy to mention that the effective transconductance seen by the degeneration resistance R_s is enhanced resulting in small voltage loss from the input to the source of M_1 . As seen from (7), the voltage gain A_V is independent of transistor parameters except for r_{o9} , and r_{o3} . In reality, R_f and R_s are chosen much smaller than r_{o9} , and r_{o3} , respectively. A_V can then be approximately expressed as,

$$A_V \cong \frac{R_f}{R_s} n \quad (8)$$

where n is the ratio (g_{m5}/g_{m3}). As a result, the gain of the circuit is stable across process corner variations. In our design, n is chosen to be equal to unity whereas the ratio R_f / R_s should be designed to implement linear-in-dB gain.

2.2. Noise analysis of the proposed VGA

Half of the differential amplifier with equivalent noise sources is shown in **Fig. 4**. The drain-source noise current generators of MOSFETs are considered. For noise sources of $M_{3,4}$ and the resistance R_s , the total output noise can be calculated as [20],

$$\overline{v_{n,out}^2} = \frac{g_{m7}^2 (R_f // r_{o9})^2 a^2}{(1 + \frac{a g_{m3} g_{m7}}{g_{m5}})^2} \overline{i_n^2} \quad (9)$$

where, $a = \left(\frac{g_{m5} r_{o11}}{g_{m5} + g_{m7}} \right) \left(\frac{g_{m1} R_s}{1 + g_{m1} R_s} \right)$ and, $\overline{i_n^2} = \overline{i_{n,M3}^2} + \overline{i_{n,R_s}^2}$; g_{mi} and r_{oi} are transconductance and output resistance of the transistor M_i .

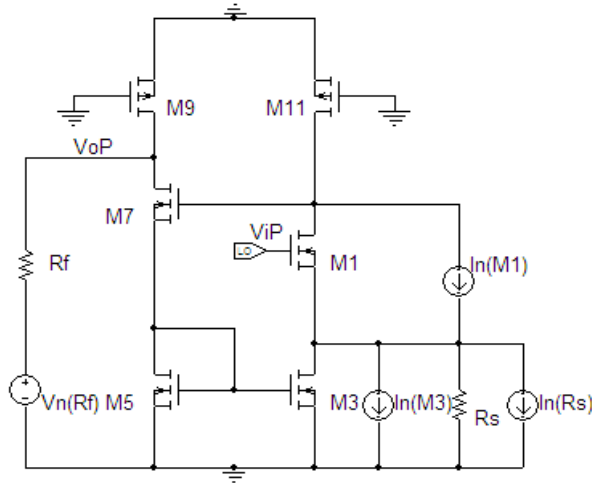


Fig. 4. Calculation of the input-referred noise of the proposed VGA-cell

Referring to the input port, $\overline{v_{n,in}^2} = \frac{\overline{v_{n,out}^2}}{|A_{v0}|^2}$, the input referred noise due to $M_{3,4}$ and R_s can be approximately expressed as:

$$\overline{v_{n,in}^2} = \left(\frac{1}{1 + \frac{g_{m7}}{g_{m5}}} \right)^2 \left(\frac{g_{m1}R_s}{1 + g_{m1}R_s} \right)^2 R_s^2 \overline{i_n^2} \quad (10)$$

The noise due to input transistor M_1 and resistance R_f can be added to estimate the total input-referred noise as,

$$\overline{v_{n,in}^2} = \frac{1}{g_{m1}^2} \overline{i_{n1}^2} + \left(\overline{v_{n,R_f}^2} + \overline{v_{n,out}^2} \right) \left| \frac{1}{A_{v0}} \right|^2 \quad (11)$$

where, $\overline{i_{n,M_i}^2} = 4kT \left(\frac{2}{3} g_{mi} \right) \Delta f + K \frac{I_{Di}^a}{f} \Delta f$, $\overline{i_{n,R_s}^2} = \frac{4kT}{R_s} \Delta f$, and $\overline{v_{n,R_f}^2} = 4kTR_f \Delta f$.

At low-gain settings, A_{v0} becomes small and so the last term in (11), defined by (10), dominates the noise performance of the circuit. As a result, R_s should be chosen small enough for good noise performance. In contrast, at large-gain settings, noise performance

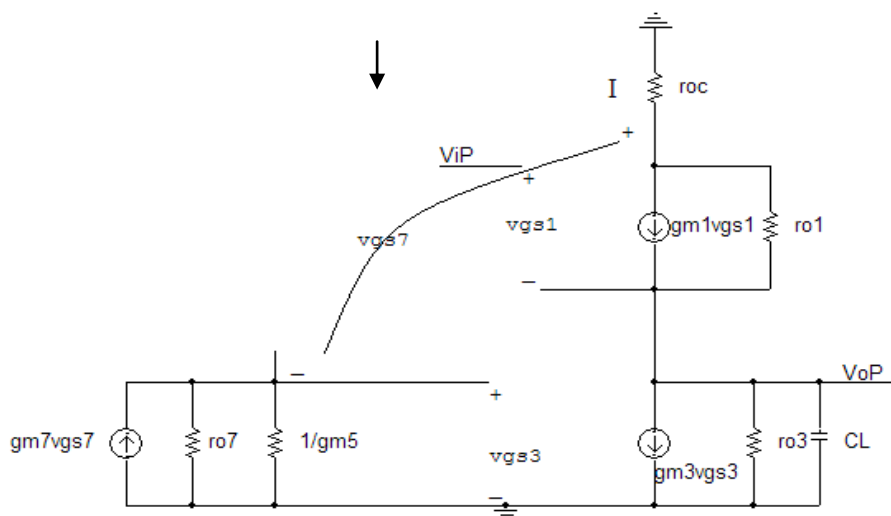


Fig. 6. Small-signal model of the proposed buffer

A similar analysis, to what has been done in Section II.A, can be conducted to calculate the output voltage gain A_v ,

$$A_v = \frac{A_o}{1 + j\omega \frac{C_L}{g_{meff}} A_o} \quad (12)$$

Where A_o is the DC gain defined by,

$$A_o = \left[\frac{\frac{g_{m1}r_{o1}r_{o3}[1 + (g_{m5} + g_{m7})r_{o7} + g_{m3}g_{m7}r_{o7}r_{oc}]}{(r_{o1} + r_{o3} + r_{oc})[1 + (g_{m5} + g_{m7})r_{o7}] + g_{m3}r_{o3}g_{m7}r_{o7}r_{oc}}}{1 + \frac{g_{m1}r_{o1}r_{o3}[1 + (g_{m5} + g_{m7})r_{o7} + g_{m3}g_{m7}r_{o7}r_{oc}]}{(r_{o1} + r_{o3} + r_{oc})[1 + (g_{m5} + g_{m7})r_{o7}] + g_{m3}r_{o3}g_{m7}r_{o7}r_{oc}}} \right] \quad (13)$$

and

$$g_{meff} = \left[\frac{g_{m1}r_{o1}r_{o3}[1 + (g_{m5} + g_{m7})r_{o7} + g_{m3}g_{m7}r_{o7}r_{oc}]}{r_{o3}(r_{o1} + r_{oc})[1 + (g_{m5} + g_{m7})r_{o7}]} \right] \quad (14)$$

If r_{oc} , r_{o1} and r_{o7} are very large and the term $r_{o3}g_{m3}$ is much greater than unity, the effective transconductance can be reduced to,

$$g_{meff} = g_{m1} \left[1 + \frac{g_{m3}g_{m7}r_{oc}}{(g_{m5} + g_{m7})} \right] \quad (15)$$

From (15), the overall transconductance is approximately improved by the closed loop gain from input to the ac current of M_3 - M_4 , through (M_1 , M_7 , M_5 , and M_3), which is very large. The overall transconductance was improved by a factor proportional to approximately $g_{m}r_{oc}$ without increasing the basic transistor size. On the other hand, the THD is superior for our proposed cell compared to the FVF cell.

3. VGA implementation and simulation results

3.1. Variable gain amplifier

The VGA is implemented in 0.13- μ m IBM CMOS process. The design equations, derived in the previous section, are used to guide our design. The VGA achieves the required bandwidth of 400 MHz with gain varying from -0.5 dB to 54 dB using 5-bits control-word. It consists of three identical VGA-cells. R_s is used to generate coarse-gain steps of 16 dB each whereas R_f is used to generate fine-gain steps of 2 dB each. Compensation capacitor array C_s has been also used in parallel with R_s to introduce a programmable zero into the transfer function that can be employed to widen out the bandwidth at large gain settings. The overall simulated variable gain amplifier current dissipation is 21 mA.

Fig. 7 shows the gain plot versus gain-control word for the simulated and analytical results equation (6); the gain is clearly linear-in-dB. There is also good agreement between analytical and simulated plots across wide gain dynamic range from -0.5 dB up to 54 dB. The insensitivity to process variation has been also studied, where there are only 0.5 dB deviations from the results of the typical mean process parameters.

Fig. 8 shows the frequency response for different gain settings. The bandwidth decreases as the gain increases, however bandwidth could be kept at its minimum value of 400 MHz by controlling the zero location without significant increase in power consumption. While the bandwidth at the maximum gain can achieve 400 MHz, the bandwidth at the minimum gain extends to 2 GHz. It is also worthy to mention that the peak occurs outside the bandwidth of interest.

The linearity performance of VGA is characterized by two-tone IIP3 test. It was measured by applying two tones of 100MHz and 120MHz at the lowest gain mode. The result is shown in **Fig. 9** where IIP3 is equal to 17.6dBm. **Table 1** compares our work against others' work in the literature. The GBW/power is taken as a figure of merit for a reasonable comparison. Our VGA shows the highest figure-of-merit. The circuit also

shows reasonable noise performance, which can be certainly improved at the expense of higher power consumption.

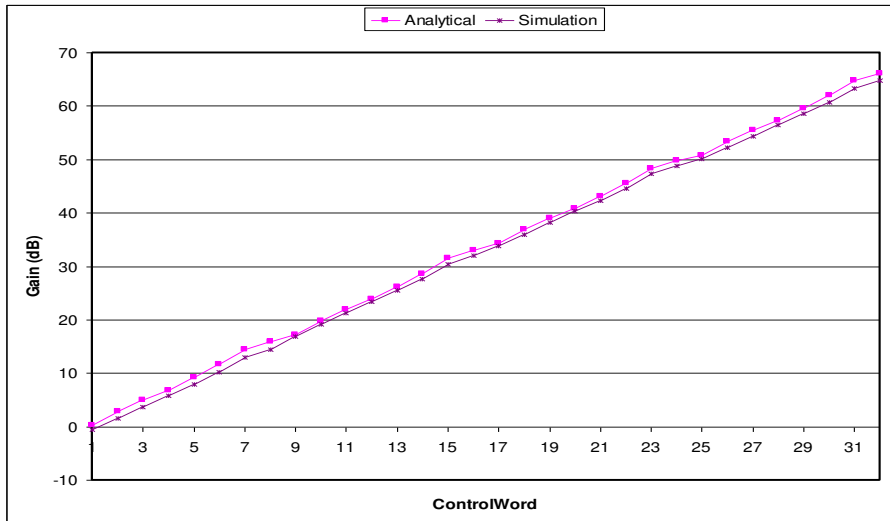


Fig. 7. Linear-in-dB gain versus control word

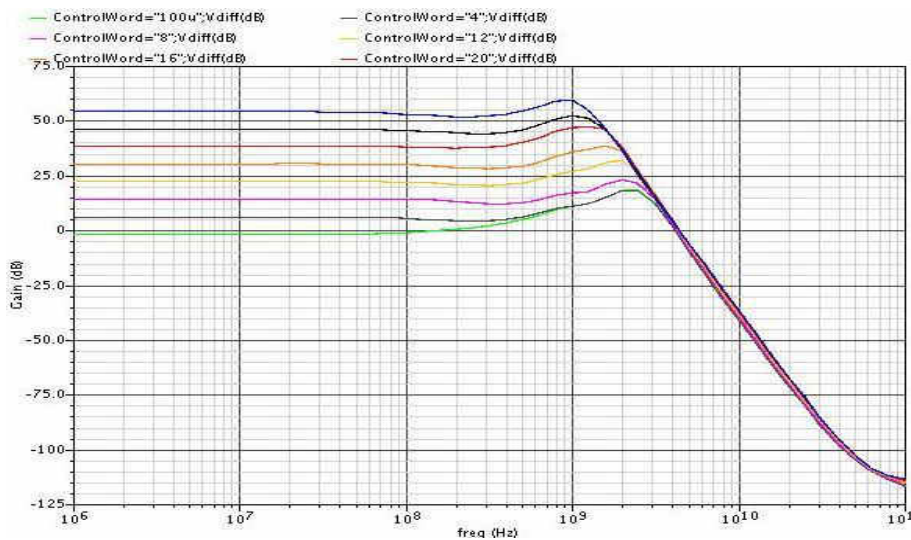


Fig. 8. Gain versus frequency for different gain settings

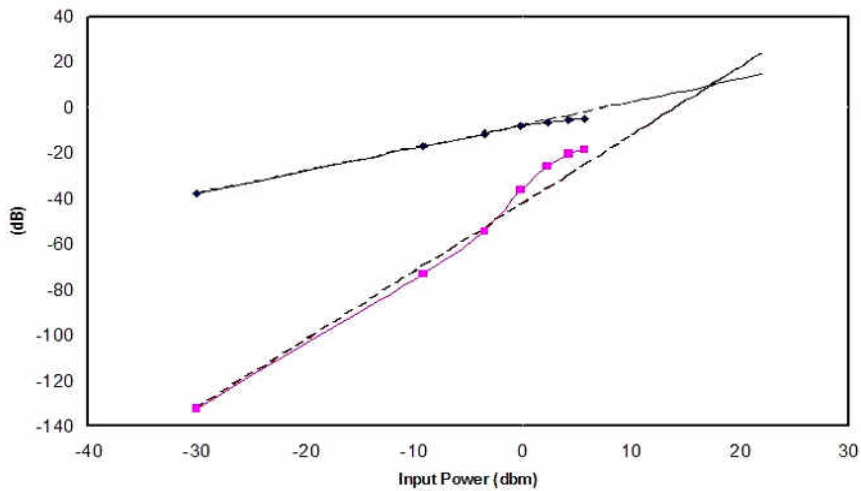


Fig. 9. The IIP3 at the lowest gain mode

Table 1
Performance summary and comparison

Parameters	[17]	[18]	[19]	[20]	This Work
Technology	0.18 μ m	0.18 μ m	0.18 μ m	0.13 μ m	0.13 μ m
Supply voltage	1.8V	1.8V	1.8V	1.5V	1.5V
Bandwidth (MHz)	450	650	400 @54dB	183 – 548	1500
Gain range	3 – 47 dB	0.7 – 60.7dB	-30 – 65 dB	-5 – 65 dB	-0.5 – 54 dB
IIP3	20dBm				17.6 dBm
Current dissipation	15mA	8.9mA	12.2mA	13.4mA	21mA
P _{diss} (mW)	27	16.02	21.96	20.1	31.5
THD @ freq=400MHz & V _{od(p-p)} =1 V					-49.47 dB @ 54 dB
					-43.26 dB @ -0.5 dB
Input referred noise					121.6 nV/ \sqrt Hz @ -0.5 Db

Parameters	[17]	[18]	[19]	[20]	This Work
GBW/Power(MHz/mW)	7518	48507	53083	48438	56103

3.2. The overall VGA

Table 2 summarizes the crucial simulation results of the overall variable gain amplifier with the output buffer at maximum and minimum gain settings. The buffer is loaded with a capacitive single-ended load of 2 pF. The noise performance of the circuit is dominated by the VGA, Table 2; the buffer noise is insignificant because of its large transconductances and so small input referred noise.

Table 2
Summary of the simulation results of the overall VGA

Parameters	@ -0.5 dB	@ 54 dB
Bandwidth (GHz)	3.5	1.5
Average Integrated Noise (nV/ $\sqrt{\text{Hz}}$)	121.6	17.4
THD (dB) @ 400 MHz and $V_{\text{odp-p}}=1$ V.	-40.04	-42.31
Power dissipation (mw)	37.5	

Fig. 10 shows the frequency response of the overall VGA at the extreme gain settings. As seen from **Fig. 10**, the frequency response extends for more than 400 MHz. Although the small-signal bandwidth can be as large as 1.5 GHz, the effective bandwidth is limited to 400 MHz only, for output voltage swing of 1 V_{dpp} with the aforementioned loading, owing to the slew-rate limitation.

4. Conclusions

This paper presents a low-voltage CMOS VGA. It achieved wide bandwidth over wide dynamic gain range from -0.5 dB to 54 dB. With this circuit topology, the gain and bandwidth can be programmed independently. The circuit has been designed and implemented using 0.13 μm IBM-CMOS process with supply voltage of 1.5 V and power dissipation of 37.5 mW to drive 2 pF single-ended capacitive loads.

This VGA can be applied to various applications, such as high performance industrial systems and baseband circuits in multi-standard wireline and wireless communications with wide bandwidth.

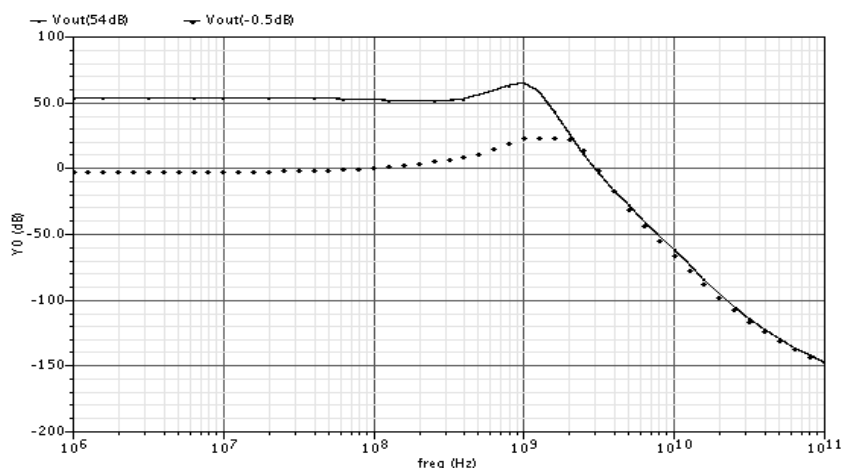


Fig. 10. Frequency response for the overall VGA

Acknowledgment

The authors gratefully acknowledge the technical support of the MOSIS Company for their support and provision of the design kit used in this work.

References

- [1] J. K. Kwon, K. D. Kim, W. C. Song, and G. H. Cho, "Wideband high dynamic range CMOS variable gain amplifier for low voltage and low power wireless applications," *Electron. Lett.*, vol. 39, no. 10, pp. 759–760, Mar. 2003.
- [2] T. Yamaji, N. Kanou, and T. Itakura, "A temperature-stable CMOS variable-gain amplifier with 80-dB linearly controlled gain range," *IEEE J. Solid-State Circuits*, vol. 37, no. 5, pp. 553–558, May 2002.
- [3] W. M. Christopher, "A variable gain CMOS amplifier with exponential gain control," in *VLSI Circuits Tech. Dig. Symp.*, pp. 146–149, Jun. 2000.
- [4] P. Huang, L. Y. Chiou, and C. K. Wang, "A 3.3-V CMOS wideband exponential control variable-gain-amplifier," in *Proc. IEEE Int. Circuits Syst. Symp.*, pp. I-285–I-288, May 1998.
- [5] M. M. Green and S. Joshi, "A 1.5 V CMOS VGA based on pseudo differential structures," in *Proc. IEEE Int. Circuits Syst. Symp.*, pp. IV-461–IV-464, May 2000.
- [6] P. Orsatti, F. Piazza, and Q. Huang, "A 71-MHz CMOS IF-baseband strip for GSM," *IEEE J. Solid-State Circuits*, vol. 35, no. 1, pp. 104–108, Jan. 2000.

-
- [7] H. O. Elwan and M. Ismail, "Digitally programmable decibel-linear CMOS VGA for low-power mixed-signal applications," *IEEE Trans. Circuits Syst. II, Analog Digit. Signal Process.*, vol. 47, no. 5, pp. 388–398, May 2000.
- [8] J. M. Khoury, "On the design of constant settling time AGC circuit," *IEEE Trans. Circuits Syst. II, Analog Digit. Signal Process.*, vol. 45, no. 3, pp. 283–294, Mar. 1998.
- [9] I. L. Abdel-Hafez, Y. A. Khalaf, and F. A. Farag, "CMOS buffer amplifier for wide bandwidth applications," *IEEE International Conference on Design and Technology of Integrated Systems in NanoScale Era (DTIS'07)*, pp. 56-59, September 2007.
- [10] R. G. Carvajal, J. Ramírez-Angulo, A. J. López-Martín, A. Torralba, J. A. G. Galán, A. Carlosena, and F. M. Chavero, "The flipped voltage follower: a useful cell for low-voltage low-power circuit design," *IEEE transactions on circuits and systems I: vol. 52*, no. 7, July 2005.
- [11] J. J. F. Rijns, "CMOS low-distortion high-frequency variable-gain amplifier," *IEEE journal of solid-state circuits*, vol. 31, no. 7, July 1996.
- [12] K. Moolpho and J. Ngarmnil, "Low voltage high-performance class-AB FGMOS buffer," *Circuits and Systems, APCCAS 2006. IEEE Asia Pacific Conference*, pp.1779 – 1782, Dec. 2006.
- [13] C.W. Lu and Y. C. Huang, "1.5 V large-driving class-AB buffer amplifier with quiescent current control," *Electronics Letters* 8th, Vol. 40 No. 1, Jan. 2004
- [14] S. Baswa, A.J. López-Martín, R.G. Carvajal, and J. R. Ramírez-Angulo, "Low-voltage power-efficient adaptive biasing for CMOS amplifiers and buffers," *Electronics Letters* 19th, Vol. 40 No. 4, Feb. 2004.
- [15] K. Hadidi, J. Sobhi, A. Hasankhaan, D. Muramatsu, and T. Matsumoto, "A novel highly linear CMOS buffer," *Electronics, Circuits and Systems, 1998 IEEE International Conference on Volume 3*, 7-10, PP. 369 - 371 vol.3, Sept. 1998.
- [16] S. Jang, S. S. Lee, S.-S. Choi, and K. C. Lee, "A CMOS Baseband Receiver for Wireless Broadband Communications," Feb. 7-10, 2010 ICACT 2010.
- [17] Y. J. The, C. F. Chung, and M. A. Arasu, "A 3-47dB gain, +20dBm IIP3, 400MHz VGA for a pulse-based UWB in 0.18 μ m CMOS," *ISIC 2009*.
- [18] J. Cheng, F.Y. Huang, L.H. Wu, Y. Tian, and N. Jiang, "A High-linearity, 60-dB Variable Gain Amplifier with Dual DC-offset Cancellation for UWB Systems," Sept. 4, WICOM.2009.
- [19] C. T. Fu and H. Luong "A CMOS linear-in-dB high-linearity variable-gain amplifier for UWB receivers," *Solid-State Circuits Conference, 2007. ASSCC '07*.
- [20] I. L. Abed-Hafez, " Design of RF –CMOS IC" M. Sc. Thesis, Zagazig University, 2009.

مكبر جهد (CMOS) ذو عامل كسب متغير لتطبيقات النطاق الترددي الواسع (UWB) عالي الخطية

ملخص:

- البحث يقدم مكبر جهد ذو عامل كسب متغير (*VGA*) للاستخدام في التطبيقات ذات النطاق الترددي الواسع. الدائرة الالكترونية المقدمة تمتاز بارتفاع قيمة سعة الجهد في المرحلة الخطية. المكبر المقترح يتركب من ثلاث مراحل متعاقبة من *VGA* مع وجود مرحلة عزل *Buffer* كوحدة خرج. الدائرة المقترحة - بهذه الموصفات- تصبح مناسبة للاستخدام في بروتوكولات الاتصالات القياسية والتي تحتاج الي حيز ترددي واسع. عند تصميم الدائرة المقترحة تم استخدام بعض الطرق لتقليل الطاقة المستهلكة كما تم تقديم وتحليل نموذج الشوشرة الذاتية الناتجة من هذا المكبر. الدائرة المقدمة تم تصميمها ومحاكاتها علي الحاسب وذلك باستخدام تكنولوجيا الـ *CMOS* و المقدمة من شركة *IBM* ذات الابعاد 0,13 ميكرو. النتائج اظهرت ان الدائرة المقترحة في هذا البحث تحقق تحسن في كثير من عوامل القياس المتبعة في الدوائر المتكاملة التناظرية وعلي سبيل المثال فهي تحقق: أوسع نطاق الدخل $DR=54.5dB$ و $IIP3=17.6dBm$ و $THD=-42.3dB$ وذلك عند جهد دخل 1,0 V من القمة للقمة وتردد يساوي (400 مجاهرتز). وعلاوة علي ذلك فإن الدائرة (*VGA*) أظهرت مشاركة قليلة بالنسبة لمتوسط الشوشرة الناتج عن الدائرة عند اقل معامل كسب ($-0.5dB$) معمل الشوشرة كان $121.6 nV/\sqrt{Hz}$.